ISOLATED NANOCRYSTALS OF INDIUM IN *KCl* CRYSTALS

S. Polosan[*], E. Apostol, E. Vasile[a], V. Topa[b]

National Institute of Materials Physics, Bucharest-Magurele, PO Box MG 7
[a]METAV, Zapada Mieilor St, no. 16-18, Bucharest-Romania
[b]Center of Advanced Studies in Physics-Romanian Academy

Metal nanoparticles embedded in KCl crystals exhibit different forms and distributions, depending on the type of metal. The nanoparticles can be efficiently studied by optical absorption on these structures, calculated from Mie theory and comparison with Transmission Electron Mmicroscopy (TEM) measurements. The TEM images provide the detailed characteristics of the structures under study. Metal crystalline particle obtained by thermal treatments of negative indium ions are spherical. The particle size distribution was determined, the standard deviation was found 1.46, and the main statistical characteristics were calculated.

1. Introduction

Based on the Mie theory of light scattering, the optical absorption of light can be calculated and, together with TEM measurements, could provide a variety of characteristics of metal nanoparticles embedded in alkali halide crystals. The formation of indium nanocrystals in KCl matrix is triggered by electron detachment of negative ions of metal, obtained by thermal treatment or by direct electrolytic coloring at high concentration of In^+ ions [1]. In the case of silver doped crystals, the metal nanocrystals present very strange arrangement [2,3], which exhibit coral- like configurations without isolated colloids.

In order to understand the process of formation of metal nanocrystals in KCl matrix, a study of the size distribution of indium colloids was performed taking into account that the melting point of bulk indium is 156 °C, much lower than the temperatures involved in electrolytic process of coloring, and in thermal treatments. In contrast with silver metal nanoparticles, which coagulate in KCl matrix into solid phase, the indium metal colloids aggregate in liquid phase and we expect that the morphology of the indium nanocrystals be quite different, i.e. exhibit separate particles. This is the advantage of applying the Mie theory of light scattering because the main conditions of this theory: separate colloids and spherical shapes are fulfiled.

The problem of the formation of metal nanocrystals of Ag, In, Cu, Zn or CdSe, CuBr, CuCl by optically induced diffusion in chalcogenide [4-6] or halide materials is of great interest due to the possible control of the electro-optical properties and applications in optoelectronics for holographic recording [7] and for rewritable optical memories [8].

The size distribution of the metal nanocrystals versus the logarithm of the particle diameter, tends to a Gaussian distribution for small size particles, whereas larger particles deviate from such a simple behavior. The geometric standard deviation, σ, as well as the analytic form of the size distribution should be of considerable interest in connection with experiments, in the case of metal nanoparticles, obtained by various techniques.

_____

[*] Corresponding author: silv@alpha1.infim.ro

2. Theory and experiments

The samples of KCl matrix with In^+ at the concentrations around 10^{17} ion/cm^3, were cleaved from the bulk crystals, obtained by Bridgman method. Electrolytic coloring process was performed using an experimental set-up described by Topa et al [9] and were made in two ways: 1) at high temperature, around 500 ^{O}C, with F centers; 2) at low temperatures, around 300 ^{o}C, without F centers. After thermal annealing, the cooling to room temperature was performed in two ways: one sample was quickly quenched and another sample was slowly quenched with ~3 ^{O}C/min.

Our team reported [1], for the first time, the formation of indium metal nanoparticles in KCl crystals, using a new technique by electron detachment of negative ions of metal (obtained by electrolytic coloring process), followed by thermal annealing and by direct electrolytic coloring at high concentration of In^+ ions (over 10^{17} ions/cm^3).

The obtained metal nanocrystals have been carefully studied through TEM and by optical scattering of light on the metal structures, using step by step Mie theory, which connects the absorption coefficient of the bulk metals with its ones dielectric constants. In fact, the theory allow us to calculate the line-shape of the absorption spectrum, starting with optical constants of bulk indium metal, which, in this case, depend on the wavelength of light, modified by the dimension of these colloids. The final form of the absorption coefficient is:

$$K(cm^{-1}) = \frac{18\pi NV}{\lambda} n_0 \frac{\varepsilon_2}{(\varepsilon_1 + 2\varepsilon_0)^2 + \varepsilon_1^2} \tag{1}$$

Under this conditions, the colloids are considered as having the dielectric constants depending on the dimension of particles and, from the absorption coefficient, it is possible to obtain the dimensions of the metal particles. The absorption results could be compared with the TEM images.

It is important to note that every deviation from these two conditions, could affect the conclusions obtained from only absorption spectra. From this reason, it is usefull to study the sphericity of the colloids from the TEM images, translating the 2D images in 3D parameters, using some mathematical aproximations.

The distribution of colloids on the TEM grid, follows the characteristics of the metal nanocrystals on the KCl matrix, with separate particles, which is the case of the Mie theory. TEM images on quickly quenched sample, was binarized and the particle size distribution was determined.

The log-normal distribution of the colloids is based on the logarithm of the volume and for spherical colloids can be written as follows:

$$f_{FN} = \frac{1}{(2\pi)^{1/2} \cdot \ln \sigma} \exp(-\frac{(\ln x - \ln \overline{x})^2}{2\ln^2 \sigma}) \tag{2}$$

where f_{FN} (x), denotes the normalized log-normal distribution function and x is the particle diameter. The relation is valid because a product of two log-normal distribution functions (LNDF) is still LNDF. More generally, the equation is valid for volumes which can be expressed in the form:

$$v = a \cdot x^b \tag{3}$$

where a and b are constants characteristic to the shape of the particles. In the following, we point out that the expression can be used even in the case of Mie theory, with good results, even when we have some deviations from the sphericity of some particles. The parameters $\overline{x}$ and σ, which define the distribution, are the statistical median and geometric standard deviation, respectively, as defined by:

$$\ln \bar{x} = \sum_i n_i \ln x_i \left(\sum_i n_i\right)^{-1} \tag{4}$$

and

$$\ln \sigma = \left[\sum_i n_i (\ln x_i - \ln \bar{x})^2 \left(\sum_i n_i\right)^{-1}\right]^{1/2} \tag{5}$$

where n_i is the number fraction of particles in an interval of the size histogram centered around x_i. It should be noted that the geometric standard deviation is dimensionless and always larger than unity. In the limit $ln\ \sigma \to 0$, the LNDF approaches the Gaussian distribution.

The moments of the LNDF allow several useful relations for particle statistics as e. g. metal nanoparticles.

The comparison of particle size distributions, estimated from experimental measurements, allows to identify the predictions about the crystallinity of the particles. For example, in the case of metal particles obtained in inert-gas evaporation [10], the geometric standard deviation was determined as

$$\sigma = 1.48 \pm 0.12 \tag{6}$$

In this case of crystalline colloidal particles, the experimental data points, exhibit a gaussian band with geometric standard deviation:

$$\sigma = 1.34 \pm 0.13 \tag{7}$$

The mercury droplets [11] have significantly wider size distribution, like as Ga droplets, which once more demonstrates that:

$$\sigma \text{ (droplets)} >> \sigma \text{ (crystallites)} \tag{8}$$

It is important now to note that, in the case of silver nanoparticles, the structures is "coral"-like in which the initial deposition during the metal nanocrystal growth, leads to nucleation at many sites of the matrix and further deposition makes these nuclei to grow mainly by adsorption of single atoms arriving by surface diffusion, also known as Ostwald ripening. The same phenomenon was revealed in the case of Au or Ag nanocrystals in which the experimental measurements of the size distribution exhibit an Ostwald ripening mechanism in the first stage, from which it was found:

$$\sigma = 1.1 \pm 0.05 \tag{9}$$

This is really true in the case of small particles in the range $0 < \bar{x} < 5$ nm. For $5 < \bar{x} < 20$ nm the Oswald ripening mechanism collapses and coalescence takes place while the particles improve their crystallinity.

3. Results

To get reliable information from TEM images, careful optimization is required concerning the boundaries between particles and conversion from pixels to nanometers. Using a typical TEM image, presented in Fig. 1, it is possible to perform a binarization in order to obtain more information about embedded nanocrystals of indium. Fig. 2 shows a typical TEM image of indium nanoclusters embedded in alkali halide crystals.
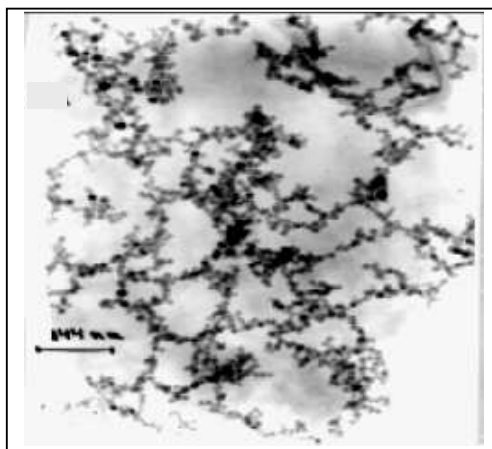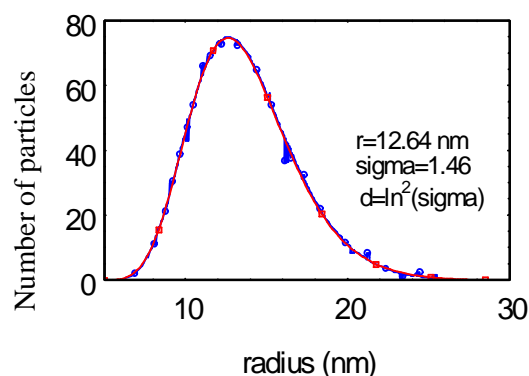
Fig. 1. TEM image of indium nanocrystals
——————— 144 nm

Fig. 2. Histogram of indium nanocrystals in KCl matrix
$y=a+b*exp(-0.5(\ln(x/c))^2/d)$,
a=-0.157, b=74.8, c=12.6, d=0.0547.

A step by step measurement of more then 600 particles from this image, allows to construct the above histogram of number of particles versus particles radius, considering spherical particles or at least ellipsoidal particles. From this histogram it is possible to determine the mean radius and the parameter σ which in our case is 1.46. The distribution function is of log-normal type.

Fig. 2 shows the histogram of computed diameters of the binarized particles obtained from the TEM image. Mean and standard deviation of every nanoparticle from TEM image, considering an area of about 600 particles are 13.44 nm and 3.583 nm. The deviation from spherical particles, is evidenced by the difference between theoretical curve based on the Mie theory and experimental curve of light scattering on the indium nanocrystals (Fig. 3).
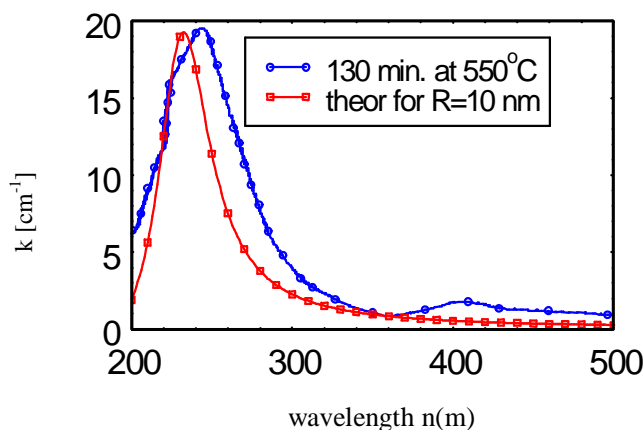

Fig. 3. Teoretical versus experimental curve.

This fact could be explained by trespassing the second condition from the Mie theory, which is applied with best results in the case of spherical particles. In order to verify the sphericity of the particles, a computation of some parameters obtained from binarized TEM images, could be useful. This binarization allow for the determination of the surface and the perimeter of every projection in 2D of the particles.

For a spherical particle, the relation between the 2D particle area projection and the perimeter of the projection circle is:

$$A \propto P^2 \qquad (10)$$

where A is the surface and P is the perimeter of the 2D projection of the particles in the TEM image. The plot A~f(P) is shown in Fig. 4 for a typical case (600 particles).

A logarithmic representation log (A)=f(log(P)), linearises this equation and the slope of this graph is 2, in the case of perfect spherical particles.
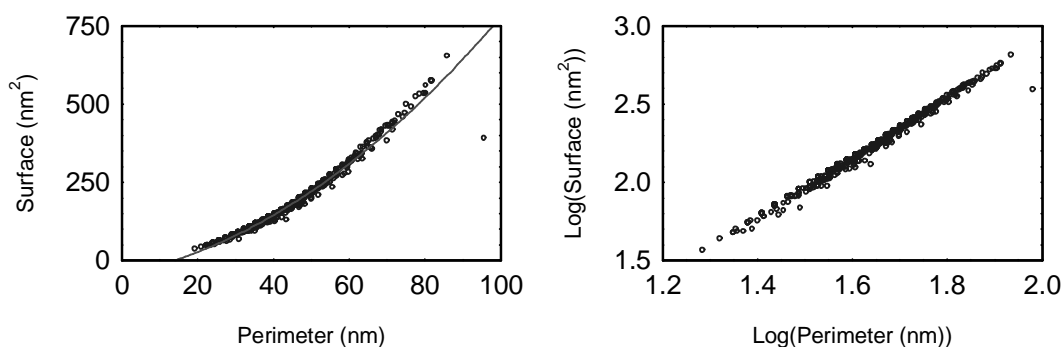
Fig. 4. Surface versus perimeter and in logarithmic scale for 600 particles.
$y = +0.0587x^2 + 2.37x - 43.9$.

From Fig. 4 it is evident a square dependence between surface and the perimeter and this fact sustains the hypothesis of almost spherical particles of indium in KCl matrix. The slope from the linear fit obtained in the logaritmic graph is 1.9.

This fact allows to conclude that some particles are not perfectly spherical, they are probably elipsoidal particles, and this feature produces difference between experimental curve of optical absorption on indium nanocrystals and the theoretical curve computed on the basis of Mie theory.

4. Conclusions

The TEM images give the posibility to extract some useful informations concerning the properties of metal nanocrystals, especially their crystallinity, the form and the size distribution. The binarized TEM images of the quickly quenched samples, show a log-normal distribution of the particles versus the radius, with a critical radius around 12 nm. The experimental histogram is well fitted with this log-normal distribution. The fit, proves that after a long thermal treatment of samples, the standard deviation is 1.46. This coresponds to the case of crystalline particles.

Due to the fact that the indium nanocrystals are obtained into the liquid phase and the surface tension plays an important role, the shape and the dimension of these structures are completely different from those of silver nanocrystals [2,3]. In the former case, the coagulation takes place in solid state aggregation in which the initial deposition leads to nucleation at many sites of matrix. Further deposition makes these nuclei to grow mainly by adsorption of single atoms arriving either by impingement or via surface diffusion, a process known as Oswald ripening [10]. In the case of indium nanocrystals the mechanism of growing is dominated by a liquid-like coalescence, a process distinct from the Oswald ripening.

The most important result of growth model based on liquid like coalescence of particles is the prediction of a log-normal distribution function for the particle size. This distribution function is obeyed very well for spherical particles.

From the experimental conditions, we believe that liquid-like coalescence is the signifiant growth mechanism, especially in the case of particles with a critical dimension between 5 and 20 nm.

As regarded the applicability of Mie theory, it is possible to compute the theoretical curve even in the case of elipsoidal particles, but there are some differences between the maxima of two curves, which do not allow to determine the critical dimension using only the scattering of light on the

metal stuctures. Using the dielectric constants of bulk indium, it is created a shift of the theoretical curve versus experimental curve, but the difference is not so large because the dielectric constant of metal indium varies very slowly with the wavelength of the scattering light.

References

[1] V. Topa, E. Apostol, S. Polosan, E. Vasile, Balkan Physics Lett. **9-2**, 101, (2000).
[2] E. Vasile, E. Apostol, M. Datcu, S. Polosan,V. Topa, J. of Cryst. Growth, **198-199**, 806, (1999).
[3] S. Polosan, E. Apostol, V. Topa, J. Optoelectron. Adv. Mater, **2(5),** 639, (2000).
[4] T. Wágner, J. Optoelectron. Adv. Mater. **4**(3), 717 (2002).
[5] D. Nesheva, J. Optoelectron. Adv. Mater. **3**(4), 885 (2001).
[6] N. Goyal, A. Zolanvari, S. K. Tripathi J. Optoelectron. Adv. Mater. **3**(3), 741 (2001).
[7] M. V. Sopinskyy, P. F. Romanenko, I. Z. Induntoryy, E. F. Venger J. Optoelectron. Adv. Mater. **3**(2), 383 (2002).
[8] T. Wágner, M. Frumar, S. O. Kasap, Mir. Vlcek, Mil. Vlcek J. Optoelectron. Adv. Mater. **3**(2), 227 (2001)
[9] V. Topa, S. Ioan, B. Velicescu, Gh. Mitroaica, Rev. Roum. Phys. **18**, 571 (1973).
[10] C. G. Granqvist, R. A. Buhman, J. of Appl. Phys. **47(5)**, 2200 (1976).
[11] C. S. Whitehead, Proc. R. Soc. **238**, 175 (1956).